NONLINEAR MID-FREQUENCY DISTURBANCE COMPENSATION IN HARD DISK DRIVES

Ying Li [*] **Guoxiao Guo** [**] **Youyi Wang** [***]

[*] *CMMS,School of Mechanical & Aerospace Engineering, Nanyang Technological University, Singapore*
Email: Liying@ntu.edu.sg
[**] *Data Storage Institute (DSI), A*STAR, Singapore*
Email:GUO_Guoxiao@dsi.a-star.edu.sg
[***] *School of Electrical & Electronic Engineering, Nanyang Technological University, Singapore*
Email: EYYWang@ntu.edu.sg

Abstract: In single-stage hard disk drives (HDDs), it is difficult to suppress mid-frequency narrow band disturbances caused by disk flutter or windage effectively. This article presents a nonlinear compensation scheme to deal with narrow band disturbance around 1 kHz. The nonlinear compensator that provides additional phase lead without degrading the magnitude characteristic is proposed. This scheme is used to compensate for phase loss due to narrow band filter and enhance the mid-frequency disturbance suppression capability. Settling performance is verified not to be degraded significantly due to harmonics from the nonlinear element. Our results show that the peak value of power spectra of NRRO due to disk vibration are decreased by 99% and position error signal 3σ value is improved 68%.

Keywords: Disk drives, Disturbance rejection, narrow band, nonlinear compensation.

1. INTRODUCTION

Disk drive areal density is increasing rapidly while price per megabyte is dropping. The servo system is a critical component for increasing the storage capacity. Ultrahigh areal density demands for stronger capability of disturbance suppression in the servo system to position the read/write head on narrower tracks.

Previous studies have shown that the major contributing factors to track mis-registration (TMR) in an HDD servo system are repeatable runout (RRO) which is synchronous with the spindle revolution and non-repeatable runout (NRRO), such as disk vibration, windage, actuator pivot and flex cable bias, which is not. NRRO imposes fundamental limitations on the viability of very high track-per-inch (TPI) drives. Among these factors, disk flutter is a dominant factor to make servo work harder to achieve high TPI drives (Ehrlich and Curran, 1999; Almaden Research Center, 2002; Guo and Zhang, 2003). In this paper, we propose a nonlinear narrow band compensation scheme to deal effectively with mid-frequency disturbances, specifically, disturbances due to disk flutter.

As disk vibration energy focuses on certain frequencies, the usual approach to suppress them

is to increase the servo loop gain at the desired frequency by inserting a narrow band filter to the servo loop (Ehrlich *et al.*, 2001; Sievers and Flotow, 1992). However, as is well known in Bode's gain-phase relationship (Bode, 1945), a slope of -$20n$ dB/decade of magnitude in a minimum-phase linear system is accompanied by a phase lag of $90n^{\circ}(n = 1, 2, 3\cdots)$. Narrow band filter is thus typically used at low frequency band, *i.e.*, the frequency of lower than 1/4 of open-loop bandwidth, due to the loss of phase caused by the narrow band filter. For those NRRO whose frequencies are far higher than servo bandwidth, narrow band filter can be carefully designed to ensure phase stabilization (Kobayashi *et al.*, 2003). Unfortunately, most of the disk flutter frequencies are in the range of mid-frequency band (500 - 2000 Hz). Inserting such a narrow band filter will thus affect the stability of the closed-loop system due to additional phase loss. Moreover, such feedback control systems typically have a poor settling performances (Wu *et al.*, 2002). Therefore, mid-frequency compensation is currently a challenging work for single-stage HDD servos.

Historically, nonlinear controllers which were developed to compensate or overcome limits in linear systems started with nonlinear servo (Lewis, 1953) or nonlinear gain element (Kalman, 1955). The idea is to shape the step response of a second-order system by varying the gain or the damping ratio during the transient response. Clegg introduced a kind of nonlinear integrator, which included a non-smooth reset element and has magnitude slope equivalent to that of a linear integrator, but with only 38° phase lag (Clegg, 1958). This improvement in phase lag over its linear counterpart was originally applied in electric servomechanism that requires high gain at low frequency range with a much reduced gain at high frequencies without loss of system stability. Later on, several other non-smooth filters which potentially break through limits of linear filters were proposed and applied in different areas (Maksimovic *et al.*, 1996; Beker *et al.*, 2001; Zheng *et al.*, 1999). Reset control was recently introduced to the HDD servo system (Wu *et al.*, 2004), where a reset integral-derivative control was developed to shorten seeking time by reducing the overshoot in track-seeking operation. Inspired by the idea of using non-smooth filters to break up Bode's gain-phase relationship, this article presents our nonlinear compensation scheme to accomplish mid-frequency disturbances suppression in HDDs.

2. NONLINEAR MID-FREQUENCY COMPENSATION IN HDD

This section will introduce the nonlinear mid-frequency compensation scheme together with the basic actuator modelling and nominal servo controller design in HDD.

2.1 Single-stage Servo System

For a single-stage actuator, the plant, *i.e.*, the object to control, includes the voice coil motor (VCM), the suspension, the slider and the head. For brevity, we use the term VCM to refer all these components. The VCM is generally modelled to be several cascade second-order sections to represent friction and mechanical resonances

$$P(s) = \prod_i \frac{K_v \omega_i^2}{s^2 + 2\zeta_i \omega_i s + \omega_i^2}, \qquad (1)$$

where K_v is a gain; ζ_i and ω_i are the damping ratio and the natural frequency for the i-th resonance. If the effect of pivot friction is ignored, the VCM typically shows a double-integrator characteristic in the low frequency range.

2.2 Nominal Feedback Controller Design

The aim of track-following servo loop is to maintain the head along the centerline of a track in the presence of various disturbances and noises. High bandwidth servo is a typical requirement for effective disturbance rejection. For a single-stage servo system, the proportional-integral-derivative (PID) controller is widely used to stabilize the servo loop. In practical implementation, the derivative section is usually replaced by a lead filter. In a PI-lead control scheme, the frequency response at mid-frequencies (near the open loop gain crossover frequency) reflects a typical lead characteristic which compensates the double-integrator behavior in VCM to have a slope of about -20 dB/decade. The integral element in the control increase the low frequency gain, in order to remove the steady-state torque disturbance at VCM input.

2.3 Nonlinear Narrow Band Compensation

Generally speaking, disturbance rejection is governed by the sensitivity function of the closed-loop system. However, for disturbances due to disk flutter whose energy concentrates in frequency regions not far away from the 0 dB crossover frequency, disturbance suppression via feedback control is not effective because of the low loop gain. Furthermore, for disturbances whose frequencies are beyond servo bandwidth, unity feedback would rather amplify it due to sensitivity "hump" in the HDD servo.

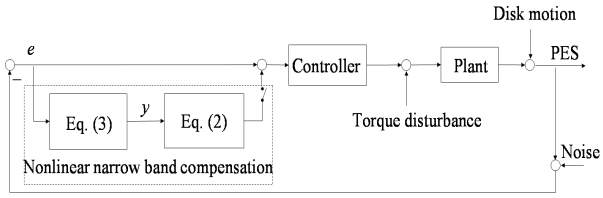

Fig. 1. The block diagram of nonlinear compensation.

Narrow band compensator can increase the servo loop gain at the disturbance frequency and cancels it through feedback loop (Sievers and Flotow, 1992). It has the following form:

$$F(s) = \frac{s^2 + 4\pi\zeta_1 fs + 4\pi^2 f^2}{s^2 + 4\pi\zeta_2 fs + 4\pi^2 f^2} \tag{2}$$

where f is the center frequency of the disturbance mode. ζ_1 and ζ_2 are the damping ratios, $\zeta_1 > \zeta_2$ is selected to produce a high gain peak value at f at the cost of phase loss after center frequency.

For disturbances which focus on mid-frequency band (around servo bandwidth), inserting a narrow band filter into the servo loop will lead to system unstable due to negative phase introduction after the center frequency. We propose a nonlinear compensation scheme that consists of two parts: nonlinear phase compensator and linear narrow band filter. The nonlinear compensator provides extra phase lead without degrading the magnitude characteristic. Fig. 1 is the schematic diagram of the proposed servo system. The nonlinear narrow band compensator is inserted into the control path in an "add-on" fashion, in which the compensator is included without requiring changes to the original controller. Because of the varying environmental conditions, limited computation power, variable structure of the typical disk drive controller and short product cycles, this is a desirable feature. On the servo transition from track-seeking to track-following, the switch is turned on to enable the narrow band compensation mode. The state-space equations for the nonlinear phase compensator is described by

$$\begin{cases} \dot{u}(t) &= -2\pi f_p u(t) + e(t) \quad e(t) \neq 0 \\ u(t^+) &= 0 \quad e(t) = 0 \\ y(t) &= k_p \dot{u}(t) + k_i u. \end{cases} \tag{3}$$

where $u(t)$ is the reset state and $y(t)$ is the output. That is, it is an ordinary lag-lead mode between reset occasions. $k_i/k_p \ll 1$ is required such that it presents a 0 dB/dec slope magnitude characteristic without phase lag in a very wide frequency band. The nonlinear mode (3) resets its lag state to zero whenever input crosses zero, which makes it arrive at zero ahead of time than the ordinary mode without reset.

As the harmonics are inevitable in the nonlinear reset mode, they will degrade the transient performance of disturbance rejection if not considered. However, from describing function analysis we will show that the nonlinear reset action shows approximate linear characteristic except around the reset frequency f_p.

For the describing function analysis of the reset action, it is supposed that the input is a sine signal:

$$x(t) = a\sin(\omega t) = a\frac{e^{j\omega t} - e^{-j\omega t}}{2j} \tag{4}$$

the output of linear lag mode $1/(s+2\pi f_p)$ without reset action is calculated by

$$\begin{aligned} y(t) &= \int_0^t e^{-2\pi f_p(t-\tau)} a\sin(\omega\tau)d\tau \\ &= \frac{ae^{2\pi ft}}{2j}\left[\frac{e^{(j\omega-2\pi f_p)t}-1}{j\omega - 2\pi f_p} + \frac{(e^{-j\omega+2\pi f_p)t}+1}{j\omega + 2\pi f_p})\right] \end{aligned} \tag{5}$$

For reset operation at zero crossing, the output is obviously periodic and have the property:

$$\int_0^{\pi/\omega} y(t)dt = -\int_{\pi/\omega}^{2\pi/\omega} y(t)dt \tag{6}$$

The DC component of the reset output is thus:

$$Y_0(j\omega) = \frac{1}{2\pi}\int_0^{2\pi/\omega} y(t)\omega dt = 0 \tag{7}$$

and the fundamental component is

$$\begin{aligned} Y_1(j\omega) &= \frac{1}{2\pi}\int_0^{2\pi/\omega} y(t)e^{-j\omega t}\omega dt \\ &= \frac{a}{j2(j\omega + 2\pi f_p)}\left(1 + \frac{j2\omega^2(1+e^{-\frac{2\pi^2 f_p}{\omega}})}{\pi(\omega^2 + 4\pi^2 f_p^2)}\right) \end{aligned} \tag{8}$$

As the Fourier Transform of the input signal (4) is

$$X(j\omega) = \frac{1}{2\pi}\int_0^{2\pi} a\sin\omega t e^{-j\omega t}d\omega t = \frac{a}{2j} \tag{9}$$

the describing function for the reset lag element is

$$\begin{aligned} E &= \frac{Y_1(j\omega)}{X_1(j\omega)} \\ &= \frac{1}{j\omega + 2\pi f_p}\left(1 + \frac{j2\omega^2(1+e^{-\frac{2\pi^2 f_p}{\omega}})}{\pi(\omega^2 + 4\pi^2 f_p^2)}\right). \end{aligned} \tag{10}$$

Further, it is piecewise analyzed as following:

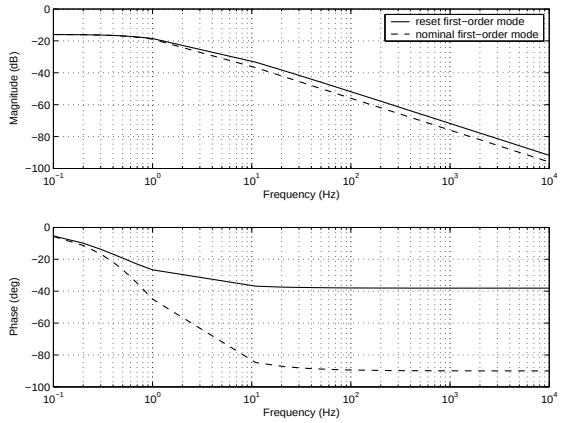

Fig. 2. The simulated describing functions of lag mode with/without reset action.

(1) When $\omega \ll 2\pi f_p$,

$$1 + \frac{j2\omega^2}{\pi(\omega^2 + 4\pi^2 f_p^2)}\left(1 + e^{-\frac{2\pi^2 f_p}{\omega}}\right) \to 1 \quad (11)$$

The reset element behaves very much like a linear element over this part of frequency range, and responses of the nonlinearly designed system is essentially the same as a linear design at this low frequency band.

(2) When $\omega \gg 2\pi f_p$,

$$1 + \frac{j2\omega^2}{\pi(\omega^2 + 4\pi^2 f_p^2)}\left(1 + e^{-\frac{2\pi^2 f_p}{\omega}}\right) \to 1 + j\frac{4}{\pi} \quad (12)$$

which has a gain of $20\log 1.62 = 4.2$ dB and phase of 51.9°. The reset behavior makes the first-order mode functions with gain of -20dB/decade roll off but with phase loss of $-90° + 51.9° = -38.1°$ at infinity high frequency range.

(3) When ω is around $2\pi f_p$,

$$1 + \frac{j2\omega^2}{\pi(\omega^2 + 4\pi^2 f_p^2)}\left(1 + e^{-\frac{2\pi^2 f_p}{\omega}}\right) \quad (13)$$

is bounded by above two limitations.

A computed transfer function of the ordinary lag mode and the simulated describing function with the reset one are shown in Fig. 2. Swept sine signal from 0.1 Hz to 10 kHz was piecewise sampled and inserted into the simulated reset model. At each piecewise frequency range, the output was online analyzed by Fourier series analysis to retrieve its fundamental component. The describing function was then obtained as the ratio of the fundamental component to input sine signal. Compared with ordinary first-order mode, gain property is preserved and shows a -20 dB/decade roll off with an extra 4.2 dB gain beyond 10 Hz. However, it introduces less 51.9° phase loss than the nominal one.

3. APPLICATION EXAMPLE

Following the design procedures for mid-frequency disturbance compensation given in Section 2, this section presents an application example in HDD track-following servo.

3.1 Parameters Selection

In our experiment, the actuator model was measured by injecting a swept sine signal into the voice coil motor (VCM) and measuring head position by a laser Doppler vibrometer (LDV), and then get the frequency response using a Hewlett-Packard dynamic signal analyzer (DSA) 35670A. The VCM model we obtained was

$$P(s) = \frac{2.097 \times 10^7}{s^2 + 150.8s + 6.317 \times 10^4} \cdot \frac{1.238 \times 10^9}{s^2 + 7037s + 1.238 \times 10^9}. \quad (14)$$

Two modes were considered for the modelling. One is the rigid-body rotation about the actuator pivot friction around 40 Hz. The other, around 5 kHz, resulted from the mechanical resonance of the actuator arm.

The typical track-following feedback controller was a PI-lead filter designed in continuous time

$$C = \frac{12.2014(s + 2651)(s + 0.6283)}{s(s + 3.977 \times 10^4)}. \quad (15)$$

and transformed to discrete time with a sampling frequency of 20 kHz. Application of the nominal controller to the plant resulted in an open-loop gain crossover frequency of 1.12 kHz with 4.04 dB gain margin and 58.2° phase margin. For the model of nonlinear narrow band compensator given above, $f_p = 1$, $k_p = 0.617$ and $k_i/k_p = 0.001$ are selected. We choose $\zeta_2 = 0.1$, $\zeta_1 = 1$ for the peak filter so that it can work for a wider frequency range to deal with disk flutter modes.

3.2 Results

To test the efficacy of nonlinear narrow band compensation, comparisons of the PES with and without nonlinear compensator were made. Settling performances are presented either to show the introduced nonlinear element does not degrade it significantly.

All the tests were performed in track following mode. With the plant model (14) and feedback controller (15), the closed-loop system was simulated using SIUMULINK. As the reason mentioned before, inserting a narrow band filter at 800 Hz into a general control system with bandwidth

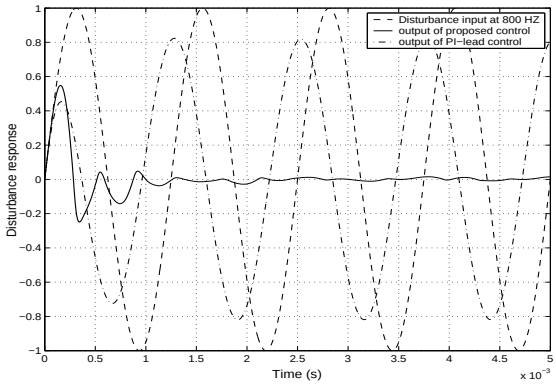

Fig. 3. Disturbance responses at 800 Hz.

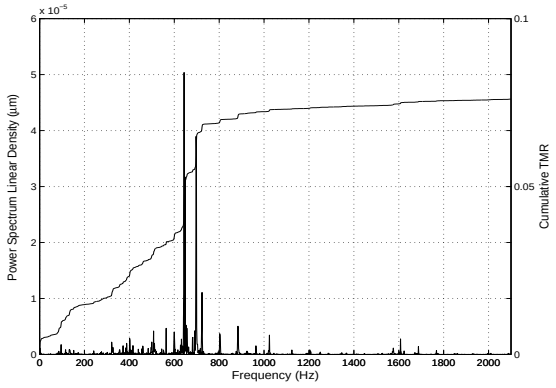

Fig. 4. NRRO power spectrum without compensation.

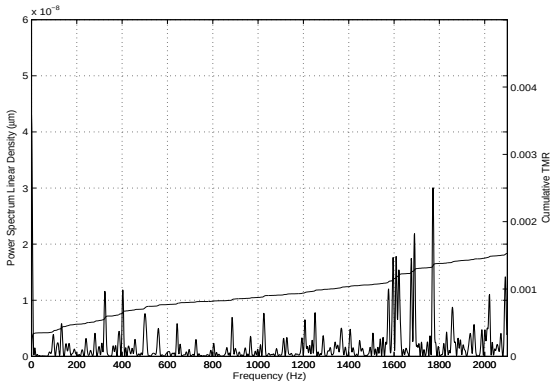

Fig. 5. NRRO power spectrum with nonlinear compensation.

of 1.2 kHz will lead to system unstable. The time traces of the PES for a 800 Hz sine disturbances with and without the proposed nonlinear compensator are given in Fig. 3. The disturbances can be almost completely removed by the nonlinear one, which is marked with solid line. However, nominal feedback servo with PI-lead controller is not quite effective to deal with such narrow band disturbance, shown as dash-dot line with a rejection of about 18%. Settling time with the nonlinear disturbance rejection scheme can also been observed with about 1.2 ms, which is not degraded seriously compared with the nominal linear feedback servo.

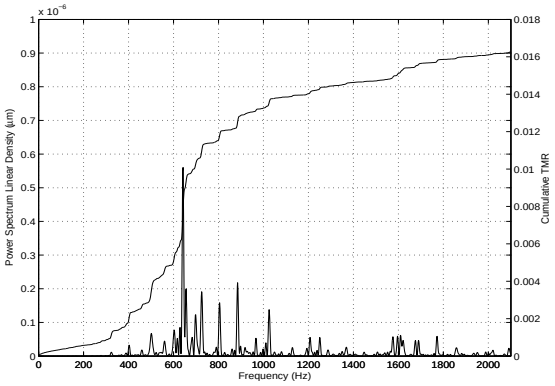

Fig. 6. NRRO power spectrum with PI-lead controller.

The NRRO disturbances for the simulations was acquired from a 3.5-inch glass disk with 4800-rpm (revolution per minute) rotation speed. Fig. 4 gives the power spectrum of raw NRRO, which is obtained by removal of RRO components in PES power spectrum. Besides power spectrum, the area beneath the power spectral density was computed to predict the cumulative TMR value, as the relation between the variance and the power spectral density of PES is given as (Lee, 2001):

$$\sigma^2(\text{PES}) \cong \frac{\sum_{i=1}^{N} \text{PSD}_i(\text{PES})}{N} \tag{16}$$

where N represents the total number of PES data points. Dominant mid-frequency modes can be seen clearly in Fig.4, especially for those at 648, 696 and 724 Hz which are excited by disk flutter. These peaks contribute to the jumps at such frequencies in the spectrum cumulative sum. Fig. 5 shows NRRO power spectrum after nonlinear narrow band compensation with one narrow band filter of central frequency $f = 700$ Hz, and peak values reduction are given in Table 1. Obviously, power spectrum linear densities at dominant mid-frequencies are greatly attenuated by using only one narrow-band filter. The cumulative sum of PES is decreased greatly in scale and also shows a flat gradual increase manner. The corresponding plot with PI-lead feedback controller is shown in Fig. 6. Feedback servo can only suppress disturbances at low frequency. For mid-frequency narrow band disturbances typically from 600 - 1000 Hz, linear feedback servo is not so effective. Fig. 7 shows the NRRO PES with the proposed nonlinear compensation in the time domain, and the corresponding control signal is shown in Fig. 8.

For the PES 3 sigma value calculated in Matlab, it is 11.31 nm for the raw PES without compensation, while 3.6 nm after the proposed compensation. The improvement is approximate to 68%.

In Table 1, power spectrum of NRRO before and after compensation are compared. For sharp

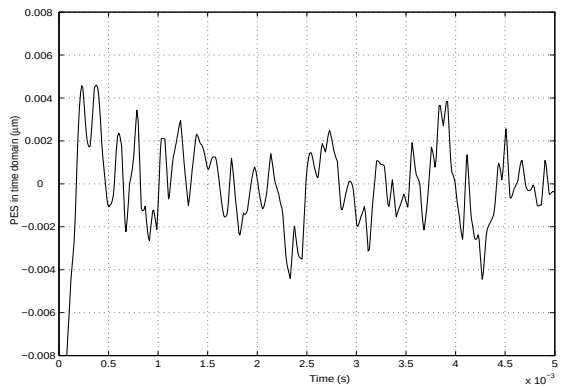

Fig. 7. The NRRO PES in time domain with the nonlinear compensation.

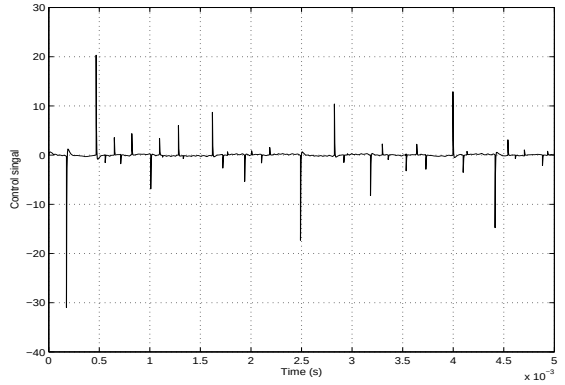

Fig. 8. The control signal in the nonlinear NRRO PES compensation scheme.

Table 1. NRRO power spectrum

Frequency	Magnitude (μm)		reduction
Hz	Before comp.	After comp.	%
598	0.4E-5	0.9E-9	99
648	5.05E-5	5.8E-9	99
696	3.9E-5	1.25E-9	100
724	1.1E-5	3E-9	99
884	0.5E-5	6.5E-9	99
1018	0.28E-5	7.2E-9	99
all frequency	0.016	0.0015	91

peaks around several main mid-frequency modes, they are almost removed completely via nonlinear narrow band compensation.

4. CONCLUSION

In this paper, we propose a nonlinear narrow band compensator which can suppress mid-frequency disturbances and thus to increase the track-following accuracy in HDDs. Simulation test showed that the proposed scheme can deal with mid-frequency disturbance effectively, and resulted in cancellation of NRRO power spectrum due to disk flutter and achieved 68% TMR performance improvement. Algorithm implementation will be carried out in our experiment setup in the future work.

REFERENCES

Almaden Research Center, Hitachi Company (2002). Introduction to feedback control with applications for HDDs. Online,http://www.hgst.com/hdd/research/images /servo loops.pdf.

Beker, O., C. V. Hollot and Y. Chait (2001). Plant with integrator: an example of reset control overcoming limitation of linear feedback. *IEEE Trans. Automat. Contr.* **46**, 1797–1799.

Bode, H. (1945). *Network Analysis and Feedback Amplifier Design.*. D. Van Nostrand. U.S.A.

Clegg, J. C. (1958). Nonlinear integrato for servomechanism. *Trans. AIEE, Part II, Appl. Ind.* **77**, 41–42.

Ehrlich, R. and D. Curran (1999). Major HDD TMR sources and projected scaling with tpi. *IEEE. Trans. Magn.* **35**, 885–891.

Ehrlich, R., J. Adler and H. Hindi (2001). Rejecting oscillatory, non-synchronous mechanical disturbances in hard disk drives. *IEEE Trans. Magn.* **37**, 646–650.

Guo, G. and J. Zhang (2003). Feedforward control for reducing disk-flutter-induced track misregistration. *IEEE Trans. Magn.* **39**, 2103–2108.

Kalman, R. (1955). Phase-plane analysis of automatic control systems having nonlinear gain elements. *AIEE Trans.* **73**, 383–389.

Kobayashi, M., S. Nakagawa and S. Nakamura (2003). A phase-stabilized servo controller for dual-stage actuators in hard disk drives. *IEEE Trans. Magn.* **39**, 844–850.

Lee, H. (2001). Controller optimization for minimum position error signals of hard disk drives. *IEEE Trans. Ind. Electron.* **48**, 945–950.

Lewis, J. (1953). The use of nonlinear feedback to improve the transient response of a servomechanism. *AIEE Trans.* **71**, 449–453.

Maksimovic, D., Y. Jang and R. W. Erickson (1996). Nonlinear-carrier control for high power factor boost rectifiers. *IEEE Trans. Power Electronics* **11**, 578–584.

Sievers, L. and A. Flotow (1992). Comparison and extensions of control method for narrow-band disturbance rejection. *IIEEE Trans. Signal processing* **40**, 2377–2391.

Wu, D., G. Guo and T. Chong (2002). Midfrequency disturbance suppression via microactuator in dual-stage hdds. *IEEE Trans. Magn.* **38**, 2189–2191.

Wu, D., G. Guo and Y. Wang (2004). Reset integral-derivative control for hdd servo systems. to appear in IEEE Trans. Contr. Syst. Technol.

Zheng, Y., Y. Chait, C. V. Hollot, M. Steinbuch and M. Norg (1999). Experimental demonstration of reset control design. *IFAC Jounral Contr. Eng. Practice* **8**, 113–120.